

Document downloaded from:

<http://hdl.handle.net/10251/119616>

This paper must be cited as:

Font-Pérez, A.; Borrachero Rosado, MV.; Soriano Martinez, L.; Monzó Balbuena, JM.; Mellado Romero, AM.; Paya Bernabeu, JJ. (2018). New eco-cellular concretes: sustainable and energy-efficient material. *Green Chemistry*. 20:4684-4694.
<https://doi.org/10.1039/c8gc02066c>

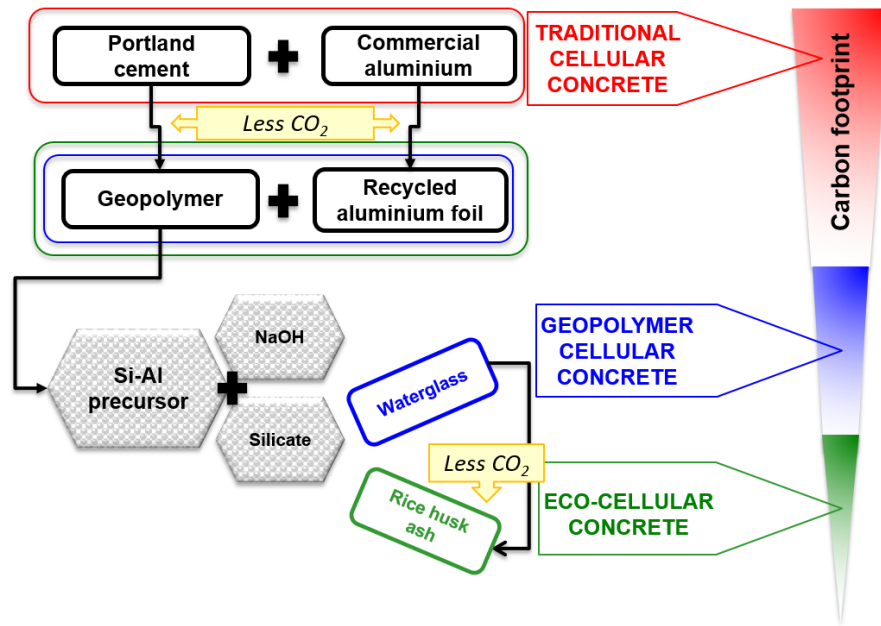


The final publication is available at

<http://doi.org/10.1039/c8gc02066c>

Copyright The Royal Society of Chemistry

Additional Information



31 **Acronyms**

32 OPC: Ordinary Portland cement

33 A: Commercial aluminium powder

34 FCC: Fluid catalytic cracking catalyst residue

35 BFS: Blast furnace slag

36 RAF: Recycled aluminium foil

37 RHA: Rice husk ash

38 **TCC**: Traditional cellular concrete (OPC + commercial aluminium powder: OPCA)

39 **GCC**: Geopolymer cellular concrete: co-milling of precursor and recycled aluminium foil (RAF):

- 40 • FCCRm: Solid resulted of the co-milling of FCC and RAF
 - 41 • FR samples: Material resulted of blending FCCRm with the conventional activating solution
 - 42
- 43 • BFSRm: solid resulted of the co-milling of BFS and RAF
 - 44 • SR samples: Material resulted of blending BFSRm with the conventional activating solution
 - 45

46 **ECC**: Eco-cellular concrete: use the RHA as silica source in activating solution (alternative activating solution):

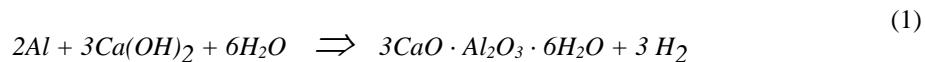
- 48 • FRR samples: Material resulted of blending FCCRm with alternative activating solution
- 49
- 50 • SRR samples: Material resulted of blending BFSRm with alternative activating solution
- 51

52 **1. INTRODUCTION**

53 Nowadays, 50% of total CO₂ emissions, 40% of used primary power and 75% of electric power
54 generation come from the building industry^{1,2}. Construction materials are an important factor of these
55 consumptions and conventional concrete is the most widely used material in this industry³. The use of
56 this material structurally goes beyond requirements in most situations.

57 Cellular concrete can be an environmentally friendly material with great insulation and low density
58 properties⁴ (300–1800 kg/m³) that yields moderate mechanical behavior⁵. It is an ordinary Portland
59 cement (OPC) based material prepared by mixing with water, and occasionally with fine aggregates
60 (sand or lightweight aggregates), with an internal air-void system formed by the addition of suitable
61 reagents. There are two methods to introduce air into the matrix: a chemical reaction in the alkaline
62 medium of metal powders (aerated concrete) or foam introduced with a surfactant addition (foamed
63 concrete)⁶. The combination of these methods has been recently studied to improve a suitable porous
64 structure⁷.

65 The addition of metallic aluminium powder is the most widespread method employed for air-bubbles
66 entrapping in traditional cellular concretes (TCC)⁸. This reagent is oxidised in an OPC alkaline medium,
67 where it comes in contact with the mixing water and the produced H₂ gas, as shown in Equation (1).

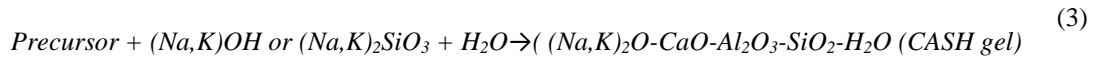
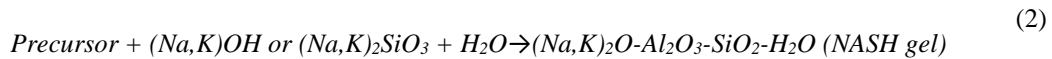


68 For many applications, TCC can provide cost and performance benefits compared with traditional
69 construction materials. As this material combines insulation properties and structural capability, it is
70 excellent for walls, floors and roofs, and its cost is sufficiently competitive with brick, wood and other
71 materials costs⁹. Furthermore, TCC is easy to cut, shape and size, and it readily takes nails or screws.
72 Common TCC applications are: pre-cast lightweight blocks, cast *in situ* lightweight walls, roof and floor
73 insulation screeds, void-filling, ground stabilisation, geotechnical and mine fill applications, and roads
74 on soft grounds^{9–11}.

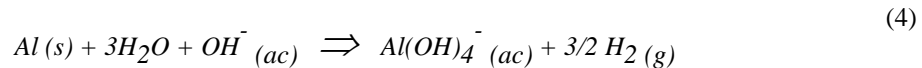
75 Thus TCC are an excellent alternative to conventional concrete in several structural situations. Even so
76 its components are actually responsible for major environmental and energetic impacts.

77 The ordinary Portland cement represents nearly 70% (by wt) of total TCC constituents (as opposed to
78 11% in conventional concrete), and the impact of this binder is well-known in terms of energy demand,
79 non renewable materials and the CO₂ footprint^{12,13}. From a chemical point of view, the application of the
80 alkali activation aiming the OPC replacement, are commonly studied as a cleaner alternative^{14–16}. The
81 alkali-activated cements or geopolymers consist of two essential components: a precursor, a mineral
82 silico-aluminate raw material, rather amorphous or vitreous; and an alkali activator, a high concentrated
83 aqueous dissolution of alkali compounds (hydroxides, silicates). The geopolymerization calls for
84 inorganic polycondensation reaction, which results in three-dimensional zeolitic frameworks¹⁷. For this
85 hardening (setting) mechanism, the first step is the precursor dissolution in contact with the OH⁻ groups
86 (that involves a high alkaline medium). The Al and Si ion are diffused or transported from the particle
87 surface inward, giving rise to a gel-like phase. And finally, a rigid chains or series of intertwined
88 tetrahedral joined by oxygen atoms are developed (species polycondensation), which must have alkaline
89 cations enough to offset the charge from the tetra-coordinated aluminium. The result is a well-stabilised,
90 stable and insoluble geopolymer binder.

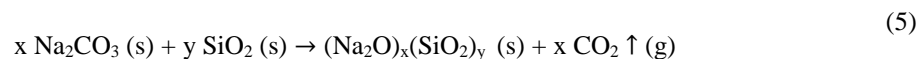
91 The mineral precursor may be a synthesized product, such as metakaolin (MK), or an industrial waste,
92 such as fluid catalytic cracking catalyst residue (FCC), fly ash or blast furnace slag (BFS). Depending
93 on the calcium content in the precursor, they can be classified according to the nature of the reaction
94 product: i) precursors with low calcium content (Equation (2)) reacts to form alumino-silicate hydrate
95 gel (NASH); and ii) precursors with high calcium content (+ CaO > 30 %, Equation (3)) reacts to form
96 calcium alumino-silicate hydrate gel (CASH).



97 The applications of geopolymer systems in manufacturing cellular concretes have emerged as a novel
 98 lightweight insulation material⁶. In the geopolymer system for cellular concrete manufacture the strongly
 99 alkaline medium make effective the aluminium oxidation thus ensuring hydrogen release as shown in
 100 Equation (4). Recent research has focused on studying these new materials. The use of BFS as a precursor
 101 to produce cellular concretes has been reported by Esmaily et al.⁷ where aluminium powder aeration was
 102 combined with the sodium lauril sulphate foaming effect. Besides, Font et al.¹⁸ have recently tested FCC
 103 as a precursor in cellular concrete aerated by using recycled aluminium foil. Both of these studies
 104 obtained excellent results thanks to their easy production and good performance without any autoclave
 105 curing process requirement.



106 The alkali solution commonly used for geopolymer activation requires silicates to obtain good-
 107 performing materials, thus the SiO_4^{4-} anion favours the formation of a denser and stronger structure¹⁹.
 108 By its important reactive part of silica, the commercial waterglass (WG) is the most common chemical
 109 reagent utilised, combined with NaOH/water solution. Nevertheless the WG is expensive (20 % of total
 110 cost of alkali activated cement production) and this synthesis represent a higher greenhouse gas emitter
 111 process (50 – 70 % of total emissions of alkali activated cements constituents)²⁰. The sodium silicate
 112 production consists on the melting of silica (SiO_2) and sodium carbonate (Na_2CO_3) until 1400°C ²¹,
 113 releasing a large amount of CO_2 (Equation (5)). For this reason, studying alternatives to replace this silica
 114 source has become the next “must have” in recent years²², and rice husk ash (RHA)²³, sugar cane straw
 115 ash (SCSA)²⁴ and glass waste²⁵ (GW) have been recently investigated.



116 Near 471 million tones of rice were produced in 2014 which the hull represents 20% by weight²⁶. The
 117 rice hull is removed and is burned to their volume reduce for disposal. This RHA contains 65 – 90 % wt
 118 % amorphous SiO_2 ²⁷. The appropriate management of rice husk and their ashes becomes an important
 119 environmental aspect because the contamination produced in farmland and watercourses in agricultural
 120 regions. The high silica content in rice husk ashes may allows their use in the new alternative geopolymer
 121 binders by its solubilisation in the activating solution yielding important environmental as well as
 122 economic profits. Recently, the use of RHA as a silica source in one-part slag alkali activated binders
 123 was introduced²⁸. These binders consist on the mix of the precursor with the solid alkali activator and
 124 water is added to initiate the reaction.

125 Another high environmental and economic impact of TCC is caused by aluminium powder
 126 manufacturing. To obtain one tonne of pure aluminium from bauxite, 15000 kWh of heat generated by
 127 electric energy is required and five tons of residues are produced^{29,30}. Apart from this, there is the
 128 additional major contribution of treatment subsequent to powder manufacturing by stamp milling, ball
 129 milling under dry conditions, wet ball milling, attrition milling and vibration milling. Since aluminium
 130 never loses its performance or strength during the recycling process, the same piece of aluminium can
 131 enter the secondary production process time and time again, which multiplies cost savings and
 132 environmental benefits. Furthermore, recycling aluminium achieves up to 95% of energy savings
 133 compared to the energy required to manufacture the same amount of aluminium to avoid depletion in

134 bauxite extraction. The result is a reduction in power from 21 kWh in the 1950s to 14 kWh in 1997 for
135 1 kg of manufactured aluminium³¹.

136 The use of alternative sources of aluminium to TCC aeration have been investigated by Araujo et al.³²
137 by incorporating aluminium recycled scrap powders. As a result, cellular concrete blocks with densities
138 less than 500 kg/m³ and low compressive strength (1.5 MPa) were obtained by an autoclaved curing
139 treatment (200°C and 10atm). These authors concluded that milling time, oxidation level and addition
140 of hard particles are the parameters that control the required density and strength properties.

141 Recycled domestic foil is another interesting alternative to use as a reagent. Annually in Europe, close
142 to 860000 tons of aluminium foil are produced, which represents a mean use of more than 26 m² per
143 inhabitant³³. The inclusion of recycled foil in the milling procedure of FCC has been recently tested by
144 Font et al.¹⁸ to use it as a raw material in new geopolymer cellular concrete (GCC) manufacturing. These
145 GCC offer several advantages over traditional OPC-based cellular concretes in terms of natural densities,
146 air-void distribution and thermal conductivity.

147 2. OBJECTIVE

148 In the present paper three steps to improve the sustainability and energy-efficiency landscape of TCC are
149 introduced, combined and discussed: i) developing a geopolymer system by using both FCC and BFS as
150 alternative precursors to replace OPC; ii) using recycled aluminium foil (RAF) to replace commercial
151 aluminium powder (A); iii) producing the activating solution by using rice husk ash (RHA) as an
152 alternative silica source for replacing commercial waterglass (WG).

153 The study of two precursors with different nature (high calcium vs. low calcium content) is essential to
154 test the material reproducibility depending on the manufacture context and resources availability. The
155 fluid catalytic cracking residue (FCC) is a low calcium content precursor whose potential as geopolymer
156 precursor was proved by Tashima et.al (2012). On the other hand, the blast furnace slag (BFS) is a high
157 calcium precursor and CaO/SiO₂ molar ratio between 0.1 and 0.6 are considered suitable for alkaline
158 activation [Talling and Bradstetr 1989). The FCC was selected to continue the previous work [Font 17]
159 where the precursor was mixed with RAF using a conventional alkali solution (NaOH + water + WG).
160 In the case of BFS there is no previous works where cellular concrete of this activated precursor was
161 aereated by RAF addition.

162 Natural density, mechanical behaviour and thermal insulation must be assessed and controlled to obtain
163 good-performing cellular concretes. Thus the proposed materials were tested to verify its resultant
164 behaviour.

165 The aim of the present investigation is the new eco-cellular concrete development, which yields good
166 performance and represents a potential solution front the traditional cellular concrete in terms of
167 environmental and energy-saving impacts (measured as carbon footprint assessment).

168 3. EXPERIMENTAL

169 3.1. Materials

170 In Table 1 an overview of the material composition of each mixture assessed in this study is shown.
171 Three cellular concrete systems were fabricated, tested and compared:

- 172 i. Traditional cellular concrete (TCC), which consists in a traditional cellular system based
173 on OPC aerated by commercial aluminium powder (A). These two materials were dry-
174 mixed manually for 1 minute to homogenise, and the mix was used as raw material (OPCA)
175 to reference material manufacture (CA).
- 176 ii. Two geopolymer cellular concretes (GCCs), designed by employing the dry solid resulting
177 from the co-milling of the precursor with recycled aluminium foil (RAF) as the raw
178 material: a) FCC with RAF (hereafter called FCCRm); and b) BFS with RAF (hereafter
179 called BFSRm). The activation of each precursor (FCC or BFS) was by using an alkali
180 solution made from sodium hydroxide and commercial waterglass (NaOH/WG).

181 iii. Two eco-cellular concretes (ECCs), prepared with the same raw material combinations as
182 GCCs (FCCRm and BFSRm), where in the alkali solution the commercial waterglass was
183 replaced with an alternative source of active silica, the rice husk ash (RHA).

Table 1 Overview of dosages.

	Mixtures	Solid phase				Liquid phase
		Precursor	Aluminium type	Pre-treatment	Raw material designation	
TCC	CA	OPC	A	Dry mix	OPCA	Water
GCC	FR	FCC	RAF	Co-milling	FCCRm	NaOH + WG
	SR	BFS			BFSRm	
ECC	FRR	FCC	RAF	Co-milling	FCCRm	NaOH + RHA
	SRR	BFS			BFSRm	

184 OPC (CEM I 52.5R) was supplied by Lafarge S.A (Puerto de Sagunto, Spain). Fluid catalytic cracking
 185 catalyst residue (FCC) was supplied by the BP Oil Company (Grao de Castellón, Spain) and blast furnace
 186 slag (BFS) was supplied as large grains by Cementval S.A (Puerto de Sagunto, Spain). The chemical
 187 compositions of OPC, FCC and BFS are summarized in Table 2.

188 Commercial aluminium powder (A) was supplied by Schlenk Metallic Pigments GmbH, whose mean
 189 particle diameter was 30 µm and the recycled aluminium foil (RAF), was supplied by the Department of
 190 Agricultural Forest Ecosystems at the Universitat Politècnica de València (Valencia, Spain). RAF was
 191 recycled after using it to cover crop glass containers in autoclaving treatments. FCC and BFS required a
 192 previous milling treatment to obtain a fine material to be used as a solid precursor^{34,35}. As previously
 193 demonstrated¹⁸ the method to incorporate RAF into the paste matrix to allow optimal reaction
 194 performance is done by blending RFA (previously reduced in small sheets: 35 mm long, 4 mm wide) in
 195 the FCC milling process. FCC and RAF sheets (0.2% wt%) were milled in a ball mill for 20 minutes to
 196 obtain a new raw material for cellular concrete manufacturing, which was designated as FCCRm (Table
 197 1). Its mean particle diameter (D_{mean}) was 18.43 µm. BFS and RAF sheets (0.2% wt%) were milled in a
 198 ball mill for 30 minutes to obtain a new raw material for cellular concrete manufacturing, which was
 199 designated as BFSRm (Table 1). Its mean particle diameter (D_{mean}) was 26.28 µm.

200 To prepare the activating solutions, the following chemical reagents were used: i) sodium hydroxide
 201 (NaOH) in the form of pellets (98% purity), acquired from Panreac S.A; ii) commercial sodium silicate
 202 (or commercial waterglass - WG), supplied by Merck-Spain (8 wt% Na₂O, 28% wt% SiO₂ and 64% wt%
 203 H₂O). Finally, rice husk ash (RHA) was utilised as an alternative silica source to produce the activating
 204 solution. This ash was supplied by DACSA S.A (Tabernes Blanques, Spain). RHA is composed mainly
 205 of SiO₂ (85.6 wt%), as seen in Table 2, and was used without milling (D_{mean} of 62.3 µm) because the
 206 particle diameter did not influence on the mechanical properties of geopolymers, as was reported by
 207 Bouzón et al.²³.

Table 2 Chemical compositions of OPC, FCC, BFS and RHA (wt%).

	SiO ₂	Al ₂ O ₃	Fe ₂ O ₃	CaO	MgO	SO ₃	K ₂ O	Na ₂ O	P ₂ O ₅	TiO ₂	Cl	LOI*
OPC	20.80	4.60	4.80	65.60	1.20	1.70	1.00	0.07	-	-	-	0.23
FCC	47.76	49.26	0.60	0.11	0.17	0.02	0.02	0.31	0.01	1.22	-	0.53

BFS	30.53	10.55	1.29	40.15	7.43	1.93	0.57	0.87	0.26	0.89	-	5.53
RHA	85.58	0.25	0.21	1.83	0.5	0.26	3.39	-	0.67	-	0.32	6.99

*Loss on ignition

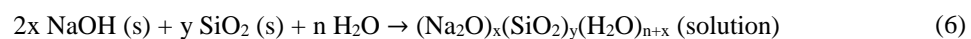
208 3.2. Methods

209 The experimental planning of this research was divided into two phases:

- 210 - First, the GCC and ECC mixes were prepared and tested by comparing the results with those
- 211 obtained for the control samples of TCC. Density, compressive strength and thermal
- 212 conductivity were studied.
- 213 - Secondly, calculation of the carbon footprint attributed to these GCCs and ECCs compared to
- 214 TCC.

215 *Samples mixing and testing*

216 In this study, to the air bubble generation in the cellular concrete matrix (TCC, GCC and ECC),
 217 aluminium powder (A or RAF in each case) was added at 0.2% by weight of the solid precursor (OPC,
 218 FCC or BFS). This reagent percentage has been commonly tested by several authors³⁶, which allows
 219 traditional cellular concrete with excellent physical and mechanical performances to be obtained. For the
 220 liquid phase, to gain an appropriate viscosity for good air-void development, the water/binder (w/b) ratio
 221 was selected f mixture. This ratio was: i) w/b = 0.5 for the TCC system (CA samples); ii) w/b = 0.6 for
 222 the FR mixes and w/b = 0.7 for the FRR mixes; iii) w/b = 0.35 and w/b = 0.45 for the SR and the SRR
 223 mixes, respectively. In the geopolymer systems, the alkali activator solution parameters that determine
 224 the amount of NaOH and silica (WG in GCC or RHA in ECC) remained constant as follows: the Na⁺
 225 molality was 7.5 and the SiO₂/Na₂O molar ratio was 1.7. These parameters have been previously studied
 226 by Payá et al.³⁷ and Bouzón et al.,²³ and were applied to GCC based on FCC by Font et al.¹⁸. The dosages
 227 for the samples based on BFS were maintained at the same proportions to make their physical and
 228 mechanical properties comparable, and in carbon footprint calculation terms. To prepare the alkaline
 229 solution, for GCC systems, NaOH and WG were mixed with water, and rest in a plastic beaker sealed
 230 with plastic film until room temperature was reached. For ECC, NaOH and RHA were mixed with water
 231 in a thermal bottle for 1 minute. To improve the solubilisation of silica in RHA by the heat released from
 232 the NaOH dissolution in water (according to Equation (6)), the thermal bottle was rest during 24 hours.



233 An AEG SBE705RE power drill connected to a paint mixer was used for sample preparation. For the
 234 cellular concrete manufacturing, the solid was mixed with its respective liquid phase (water for TCC or
 235 alkaline reagent for GCC and ECC) for 190 seconds in the TCC mixes and for 30 seconds for the
 236 dissolution, plus 90 seconds when the solid blend was incorporated into the GCC and ECC mixes (the
 237 total mixing time was 120 seconds). The alkali activated systems required a shorter mixing time because
 238 the high alkalinity medium provided a quick aluminium powder reaction compared to OPC systems. No
 239 compacting treatment was carried out to avoid gas escaping from the aerated concrete during the setting
 240 process. For each resulting concrete twelve 10x10x10 cm³ cube specimens were moulded and cured at
 241 23°C and 100% RH for 24 h when the free surface of cubes had to be cut with a saw blade. Then
 242 specimens were demoulded and kept in a wet chamber (23°C and 100% RH) until testing.

243 By considering natural density (ρ) to be the volumetric mass density (mass per unit volume), it was
 244 determined by means of the weight of the 10-cm cubic samples before compressive strength testing. The
 245 compressive strengths of the cellular concretes were obtained by an INSTRON 3282 universal testing
 246 machine. The compressive test was performed after 7 and 28 curing days. Tests were carried out on four
 247 cubic specimens (10x10x10 cm³) for each curing time, and averages and standard deviation values were
 248 calculated.

249 A KD2-Pro handheld device (Decagon Devices Inc.) was employed to determine thermal conductivity.
250 Thermal measurements were taken by a thick (6 cm long, 3.9 mm diameter) single RK-1 sensor based
251 on the dual needle probe system (transient line source method) according to ASTM D5534-08³⁸ and
252 Standard IEEE 442-1981³⁹. Before taking measurements, a standard (RH-1-01116, 0.387±10% W/mK)
253 was used to verify the sensor's good performance. Room temperature thermal conductivity was measured
254 on four cubic specimens (10 x 10 x 10 cm³) of each formulation. A rotary hammer bit to drill pilot holes
255 (6 cm long, 4 mm diameter) was necessary to accommodate the RK-1 sensor.

256 *Carbon footprint calculation*

257 The calculations and comparisons among the CO₂ emissions related to the TCC, GCC and ECC systems
258 were made.

259 To that end, the International Panel on Climate Change (IPCC) Guidelines for National Greenhouse Gas
260 Inventories was followed⁴⁰. The general methodology employed to estimate the CO₂ emissions
261 associated with a particular process involves the product of activity level data: the amount of the material
262 processed or the amount of energy consumed, and an associated emission factor per unit of
263 consumption/production according to:

$$E_i = A_i EF_i \quad (7)$$

264 Where E_i = the process emission (kg) of CO₂ from each component or operation 'i'; A_i = the amount of
265 activity or processed material 'i'; and EF_i = the emission factor associated with the CO₂ per unit of
266 activity or process material 'i'.

267 Two different phases were assessed: i) Phase 1: emissions associated with each single material which
268 forms a cellular concrete (called emissions associated with the components, E_C); ii) Phase 2: emissions
269 associated with the cellular concrete manufacture considering laboratory conditions (milling and mixing
270 procedures) (E_M). The carbon footprint calculation result was calculated as the sum of the emissions from
271 its two phases (Equation (8)).

$$E_{TOTAL, i} = E_{C, i} + E_{M, i} \quad (8)$$

272 Where "i" is the sample (CA, FR, FRR, SR or SRR).

273 Calculations were made to obtain, in the same context (laboratory conditions), 1 m³ of each material. For
274 the volume of manufactured materials to be comparable, their same density was considered herein (600
275 kg/m³). By considering this aspect, the currently commercial cellular concretes with the proposed
276 alternatives and the same properties were compared.

277 The amounts of the solid precursor, combined water and solid alkali compounds present in each mix
278 were obtained from the thermogravimetric analysis (TGA) with a Mettler-Toledo TGA 850. The
279 obtained DTG curve provides the amount of water chemically combined in the samples in weight
280 percentage. The weight difference corresponds to the solid phases: precursor, Na₂O and SiO₂. For a given
281 dosage (w/b ratio, Na⁺ molality and SiO₂/Na₂O molar ratio) the solid phases proportion in the samples is
282 constant, and the amount of the precursor to obtain a cellular concrete with a given density can be
283 determined by the following relationships showed in Figure 1.

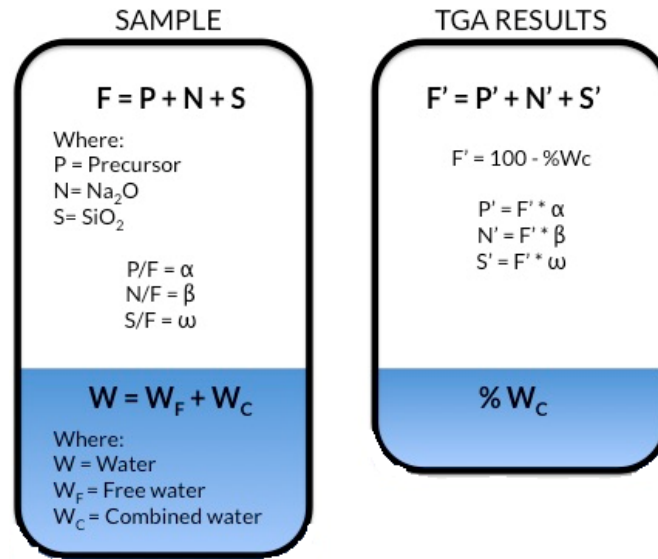


Fig 1. Methodology for obtaining the dosages of cellular concretes from TGA results.

284 **4. RESULTS AND DISCUSSION**

285 **4.1. Physical and mechanical characterisation**

286 Table 3 shows a summary of the results obtained in the experimental section of the cellular concretes
287 studied in this work.

Table 3: TCC, GCC and ECC properties obtained from tests

	Natural density (kg/m ³)	Compressive strength (MPa)		Thermal Conductivity (W/mK)
		7d	28d	
CA	618 ± 2	4.5 ± 0.4	6.5 ± 0.4	0.182 ± 0.001
FR	813 ± 2	3.5 ± 0.2	4.3 ± 0.4	0.083 ± 0.003
FRR	782 ± 4	2.6 ± 0.4	3.2 ± 0.3	0.113 ± 0.005
SR	474 ± 4	1.6 ± 0.5	2.6 ± 0.2	0.281 ± 0.007
SRR	611 ± 4	3.2 ± 0.2	4.6 ± 0.3	0.224 ± 0.007

288 The TCC based on OPC and commercial aluminium powder (A), CA sample, had a natural density of
289 618±2 kg/m³ and its compressive strength yielded 4.5 and 6.5 MPa for 7 and 28 curing days, respectively.
290 These values are in line with those reported in the literature, where values of 600 kg/m³ are related with
291 compressive strengths of 2.8 to 6.3 MPa at 28 days^{5,41}.

292 For the GCC system, activated by a traditional alkali solution (NaOH, commercial waterglass and water),
293 replacing the commercial aluminium powder (A) by recycled aluminium foil (RAF) allowed interesting
294 cellular systems to be obtained.

295 With the addition of RAF, the FR resultant material yielded a natural density of 813±2 kg/m³ (31.6%
296 higher than the TCC system). Compressive strength varied from 3.5 after 7 days to 4.3 MPa after 28
297 days. In contrast with its natural density value, this mechanical behaviour represents a 34.1% reduction
298 compared to the TCC system. These results do not agree with those reported by Font et al.¹⁸ in their
299 previous research work where the geopolymer samples with FCC allowed the natural density to lower
300 and yielded a compressive strength gain compared to the TCC systems. It could be attributed to the
301 difference in the w/b ratio and to specimen dimensions. Since cellular concretes should flow to avoid
302 compaction or vibration, for a larger volume material the required w/b ratio would have to be equal 0.6.
303 This value involves higher fluid consistence and, consequently, extends the time spent on gaining matrix
304 stability, which allows gas entrapping. During this time, most of the generated gas from the aluminium
305 reaction was not entrapped, and the resultant void-system in the paste produced a poorer performing
306 system in terms of natural density and strength. In a previous research, for foamed concrete, Nambiar et
307 al.⁴² and Zhang et al.⁶ established that a controlled w/b range is required to develop an optimal and stable
308 void system in the matrix.

309 With the use of BFS precursor, the RAF reaction into the cementitious matrix involves an effective
310 cellular structure and the resultant average density of the SR samples was 474±4 kg/m³ (23.3% lower
311 than CA). The mechanical strength was 1.6 MPa after 7 curing days, and 2.6 MPa after 28 days. The
312 strength value was 60.9% lower than the CA compressive strength. This expected behaviour in the SR
313 samples agrees with the linear relationship between density and compressive strength in cellular concrete
314 systems. In this case, given the low w/b ratio of 0.35, most of hydrogen gas was entrapped in the matrix,
315 which led to lower natural density compared to TCC.

316 The ECC systems, where the traditional activating solution (NaOH, commercial waterglass and water)
317 was replaced by a mixture of NaOH and RHA in water, showed interesting behaviour. Concrete prepared
318 with FCC (FRR) had natural density of 782±4 kg/m³, which was 26.6% higher than CA, and was similar
319 to the FR sample. Compressive strength yielded from 2.6 MPa after 7 curing days to 3.2 MPa after 28
320 curing days. This mechanical behaviour was 51.3% lower than that obtained in the CA samples which,
321 as with the FR samples, contrasts with the strength-density linear relationship usually found in cellular
322 concretes. This can be explained by the same discussion as that mentioned above based on the w/b ratio.
323 In the BFS-based ECC system (SRR samples), the results showed an interesting evolution when WG

324 was replaced by RHA and its natural density was similar to that obtained in the CA samples (611±4
325 kg/m³). Compressive strength yielded 3.2 MPa after 7 days of curing and 4.6 MPa after 28 days, values
326 significantly higher than those obtained for SR concrete.

327 These results highlighted that the amount of silica soluble from RHA allows obtain an appropriate alkali
328 activator reagent, which potentially reacts with the precursors forming the cementing gels. In any case,
329 the use of an aerating agent as well as replacing the commercial aluminium powder with recycled
330 aluminium foil (RAF) allowed good-performance cellular concretes to be prepared.

331 Regarding thermal properties (Table 3), the traditional cellular samples (CA) yield 0.182 W/mK. With
332 the alternative geopolymer systems, the highest value was obtained for SR sample (0.281 W/mK)
333 followed by SRR (0.224 W/mK), FRR (0.113 W/mK) and finally FR, which yield the lowest value (0.083
334 W/mK). With the results obtained herein, we highlight the good insulation performance of the studied
335 alternative cellular materials. Specifically, regards to FCC based cellular concretes, the lowest thermal
336 conductivity was obtained despite they had the highest natural density. This behaviour suggested that the
337 pore distribution of aerated system was very advantageous when FCC is used as precursor.

338 A clear visual comparative of the physical properties is shown in Figure 2. The following coefficients
339 (Equations (9) (10) and (11)) were determined by analysing the results of the physical tests (density,
340 compressive strength and thermal conductivity), and after considering the ratio between each alternative
341 cellular concrete based on waste precursors and recycled aluminium foil (GCC and ECC) respect the
342 TCC system based on OPC and commercial aluminium powder. These coefficients allowed us to
343 compare the potential of the GCC and ECC systems in terms of the selected properties.

$$\vartheta_d = \frac{\rho_x}{\rho_R} \quad (9)$$

Where:

ϑ_d = Density ratio coefficient

ρ_x = Density for the alternative cellular concrete (FR, FRR, SR or SRR)

ρ_R = Density for the TCC (CA)

344

$$\vartheta_s = \frac{r_x}{r_R} \quad (10)$$

Where:

ϑ_s = Compressive strength ratio coefficient at 28 curing days

r_x = Compressive strength for the alternative cellular concrete at 28 days (FR, FRR, SR or SRR)

r_R = Compressive strength for the TCC (CA) at 28 curing days

345

$$\vartheta_t = \frac{k_x}{k_R} \quad (11)$$

Where:

ϑ_t = Thermal conductivity ratio coefficient

k_x = Thermal conductivity for the alternative cellular concrete (FR, FRR, SR or SRR)

k_R = Thermal conductivity for the TCC (CA)

346

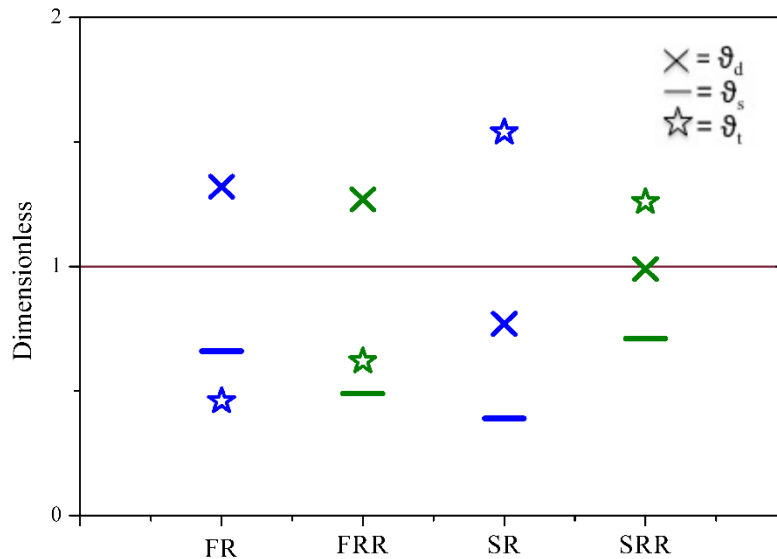


Fig 2. Density, compressive strength and thermal conductivity ratio coefficients for the GCC and ECC systems.

347 The horizontal solid line shown in Figure 2 represents the unit value of the ratio coefficients. The values
 348 of ϑ_d , ϑ_s and ϑ_t above the line denote that the corresponding property of the material is higher than that
 349 for the CA reference, and the values below the line mean that it is lower than the CA reference one.

350 Since, a good performance of cellular concrete involve its low density, moderate compressive strength
 351 and low thermal conductivity, from Figure 2 it is possible to denote that:

- 352 • FCC samples are denser than the reference material, being the FRR density ratio slightly closer
 353 to the unit. Respect to the use of BFS as the precursor, the SR density is below the line
 354 (corresponding to the lower value), while the SRR density coefficient is the closer one of the
 355 solid line. As for FCC samples as for BFS the density coefficients are closer to the unit when
 356 RHA is used to replace the silica from WG.
- 357 • Analysing the compressive strength ratio coefficients it is clearly highlighted the directly
 358 relation with the density for FCC samples and the inverse relationship for BFS samples. The
 359 strength values for all alternative cellular concretes evaluated were lower than that obtained for
 360 CA.

- 361 • The lowest thermal conductivity values were yielded for system in which FCC is used as the
 362 precursor despite their density values.
 363 • By considering the three physical properties coefficients, the use of RHA involves the
 364 corresponding ratio coefficients closer than the unit (solid line).

365 **4.2. Carbon footprint calculation**

366 The components and manufacturing process for each cellular concrete, considered with the CO₂
 367 emissions calculations, are summarised in Table 4.

Table 4: Overview of each cellular concrete system component (C) and manufacturing process (M) for carbon footprint calculation.

	TCC	GCC		ECC		
	CA	FR	SR	FRR	SRR	
C	Solid phase	OPCA	FCCRm	BFSRm	FCCRm	BFSRm
	Liquid phase	H ₂ O	NaOH/WG/H ₂ O		NaOH/RHA/H ₂ O	
M	Mix	Milling + Mix				

368 Two phases for three different cellular systems were assessed, which were as follows.

369 Phase 1: Emissions associated with components (E_c)

370 Table 5 shows the resultant dosage of the CA, FR, SR, FRR and SRR cellular concretes by considering
 371 that these must have a density of 600 kg/m³ (dry conditions).

372 If we consider a CA sample with a density of 600 kg/m³, it represents 600 kg of total weight, formed by
 373 OPC and combined H₂O. This water is chemically combined to form the typical CSH, ettringite, CASH,
 374 CAH and CH products, among others, from hydration reactions (C-CaO; S-SiO₂; A-Al₂O₃; H-H₂O). The
 375 total mass loss observed on the DTG curve (35–600°C temperature range) of the CA paste (20.32%)
 376 (Figure 3) represents this chemically combined water. This means that 79.68% of the sample corresponds
 377 to OPCA.

378 The emission factor associated with clinker production was 1 kg of CO₂ per kg of cement^{3,15,43}. If we
 379 consider that the used OPC was 95% composed of clinker, the emission factor adopted for the calculation
 380 would be 0.95 CO₂/kg. Zero emission was considered for water supply. Regarding the emission
 381 associated with the aerating agent, the corresponding factor for gas generator production was 11.5 kg
 382 CO₂ per kg of A. In this case, the emission factor related to aluminium powder metallurgy processing
 383 (air or gas atomisation) was not considered because this value was not available from the consulted
 384 databases. Finally by using Equation (7), the total CO₂ emissions associated with components per m³ of
 385 TCC were calculated (E_{C,CA}), resulting 467.0 kg CO₂/m³ CA.

386 For the GCC samples, an FR sample with a density of 600 kg/m³ represented 600 kg of the resultant
 387 weight, formed by FCC, Na₂O, SiO₂ and chemically combined water (to form NASH gel). By the total
 388 mass loss from the DTG curve (14.09%) (Figure 3), the chemically combined water was determined.
 389 From the alkaline solution stoichiometry (Na⁺ molality=7.5 and SiO₂/Na₂O molar ratio = 1.7) and the
 390 w/b ratio (0.6), the Na₂O and SiO₂ percentages were constant compared to the solid precursor. The same
 391 ratios were considered with the SR sample, which yielded a total mass loss of 14.19% on the DTG curve
 392 and had the same stoichiometry for the activating solution, with a w/b ratio equal to 0.35.

393 Since FCC and BFS are industrial wastes and RAF was from recycled supply, no emission associated
 394 with them was considered. The manufacture of NaOH and commercial waterglass was taken into account
 395 (no emission associated with water supply). Both emission factors, which corresponded to NaOH and

396 WG, were obtained from the SimaPro7.1 program databases (demo version, Pré Consultants Company
 397 of The Netherlands, LCA software specialist). The emission factors were 1.12 kg CO₂ of NaOH and 1.2
 398 kg CO₂ per kg of the commercial waterglass solution. Finally by using Equation (7), the total CO₂
 399 emissions associated with components per m³ of each GCC were calculated, which were E_{C,FR} = 322.5
 400 kg CO₂/m³ for FR and E_{C,SR} = 207.7 kg CO₂/m³ for SR.

401 In the ECC systems, WG was replaced with RHA. The solid components of the FRR and SRR samples
 402 were the same as for FR and SR, respectively, and the alkali solution based on H₂O, NaOH and RHA
 403 composed the liquid phase (Table 4). The amount of each component required in the 600 kg/m³ FRR or
 404 SRR dosages was obtained by the same means as for FR and SR, explained above from the
 405 thermogravimetric data and stoichiometry of the activating mixture (see Table 5 and Figure 3).

406 According to the above E_{C,FR} and E_{C,SR} calculations, no emissions associated with FCC, BFS and RAF
 407 were considered. Moreover, RHA is an agricultural waste, thus no emissions associated with it were
 408 considered. In this case, only the CO₂ emissions from NaOH manufacturing were contemplated. Thus
 409 the E_{C,FRR} and E_{C,SRR} values were 88.3 and 65.8 kg CO₂/m³, respectively.

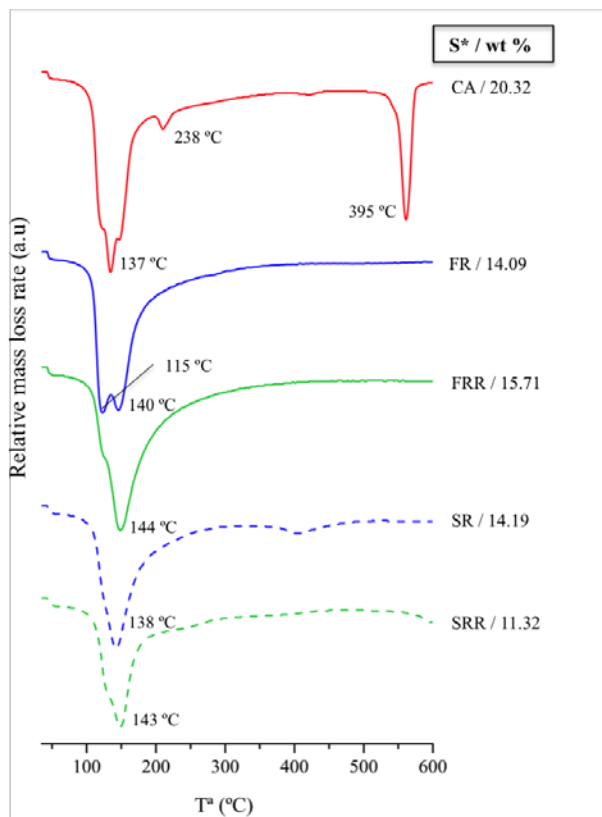


Fig 3. The DTG curves of the CA, FR, FRR, SR and SRR samples.

S/wt % = sample/total mass loss % per weight*

410

411

412

413

414

Table 5: Dosages of CA, FR, SR, FRR and SRR samples to obtain a cellular concrete with a density of 600 kg/m³.

CA		FR		SR		FRR		SRR	
		FCC	397.4kg	BFS	438.8kg	FCC	375.6kg	BFS	435.2kg
OPC	480.0kg	RAF	0.8kg	RAF	0.9kg	RAF	0.8kg	RAF	0.9kg
A	0.9kg	H ₂ O	95.4kg	H ₂ O	61.4kg	H ₂ O	363.9kg	H ₂ O	195.8kg
H ₂ O	240.0kg	NaOH	48.5kg	NaOH	31.2kg	NaOH	78.9kg	NaOH	58.7kg
		WG	223.5kg	WG	144.0kg	RHA	76.7kg	RHA	57.1kg

415 Figure 4 shows the percentage of contribution to CO₂ emissions from the components and the percentage
 416 that represents each component in the final dosage material.

417 It is noticeable in the CA samples, that the CO₂ emissions coming from the OPC (whose are 66.6% of
 418 the total dosage) represent nearly 97% of the total component emissions, and the remaining 3% is caused
 419 by the use of powdered aluminium (which represents merely 0.16% of the dosage).

420 The application of both proposed GCC systems yielded a marked E_C reduction compared to the TCC
 421 system emissions. E_{C,FR} and E_{C,SR} gave 30.9% and 55.5% less than E_{C,CA}, respectively. We highlight that
 422 in these two GCC systems, the emissions from the WG manufacturing, represented nearly 83% despite
 423 this component is in 29.2% and 21.3% in the FR and SR dosages, respectively. The remaining 17% of
 424 E_C was related to NaOH manufacturing (Figure 4).

425 Finally regarding ECC (where the total component emissions were associated with NaOH), for the FRR
 426 samples the NaOH dosage represented 9.9% of the total weight and the resultant E_{C,FRR} was 88.3 kg
 427 CO₂/m³ FRR. This E_{C,FRR} was 72.6% lower than E_{C,FR} and 81.1% lower than E_{C,CA}. For the SRR samples,
 428 the NaOH dosage represented 7.8% of the total weight and the resultant E_{C,SRR} was 65.8 kg CO₂/m³
 429 SRR. This E_{C,SRR} was 68.3% lower than E_{C,SR} and 85.9% lower than E_{C,CA}.

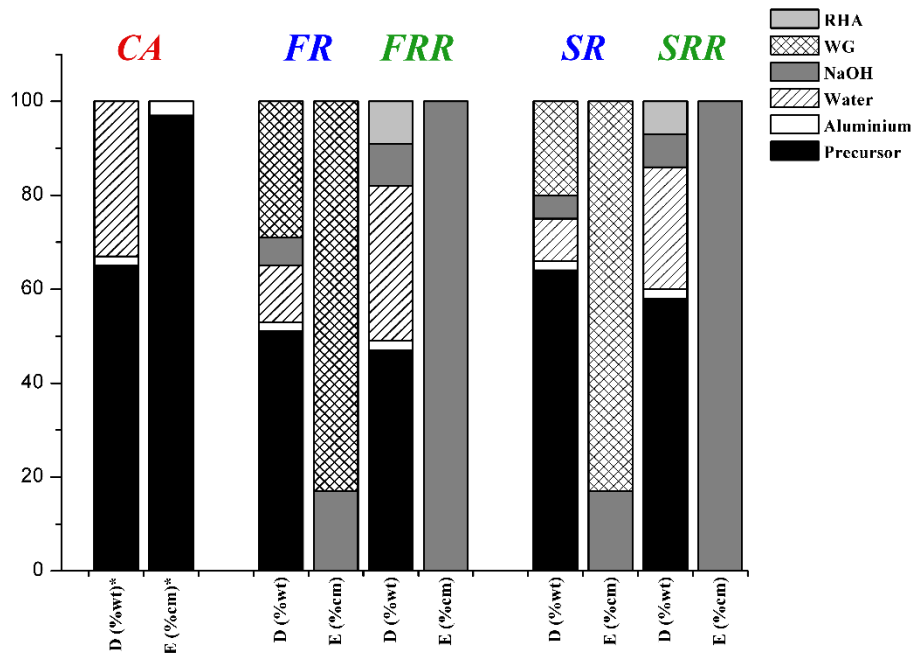


Fig 4. Comparison of the contribution percentage to the CO₂ emissions from components (* E (%cm):) and the percentage that represents each component in the final dosage material (D (% wt): weight percentage) for the CA, FR, FRR, SR and SRR cellular concretes.

430 It can be focus this noticeable reduction in CO₂ emissions in relation to the cellular concrete components
 431 mainly on the replacement of chemically synthetic reagent WG. The synthesis of commercial waterglass
 432 consists in the reaction of quartz and sodium carbonate, which is carried out at high temperature (above
 433 1300°C) and involves CO₂ emissions from sodium carbonate decomposition (Equation (5)) and the
 434 energy required to heat the quartz/Na₂CO₃ mixture in a furnace. These results agree with the statements
 435 found in several works which have centred on searching for an alternative silica source in alkali-activated
 436 materials ^{21,43,44}.

437 It is worth considering that the aluminium contributions in emissions were much lower: 3% for TCC
 438 production, and were completely null for the alternative GCC and ECC systems. However, we must take
 439 into account that no aluminium powder metallurgy processing was considered for TCC production. In
 440 any case, the way proposed to include RAF in the FCC/BFS milling process became a new ecological
 441 material to remove the emissions associated with this commercial gas-generating reagent.

442 Phase 2: Emissions associated with the manufacture process (E_M)

443 The manufacturing of TCC, GCC and ECC involves assessing three different activities: i) the pre-
 444 treatment of raw materials; ii) the mixing procedure; iii) the curing procedure. The evaluated cellular
 445 concrete samples were cured at room temperature and, for this reason, only the first two activities were
 446 considered herein. Additionally with ECC systems, no emissions associated with dissolution
 447 preparations in a thermal bottle were produced. Since no industrial process exists for GCC and ECC
 448 production, calculations were made by considering the same manufacture conditions as those used to
 449 produce concrete in a laboratory.

450 The raw materials used to prepare TCC (OPC and A) have an industrial manufacture system and their
 451 pre-treatment was not necessary. For the GCC and ECC systems, as in Section 2.2 “Materials” was
 452 explained, FCCRm and BFSRm solid mixes were achieved by the grinding treatment. To obtain FCCRm,
 453 FCC and RAF were co-milled in a ball mill at 0.3 kW electric powers, and capacity was 300 g and

454 grinding time was 20 minutes. The same ball mill was used to obtain BFSRm but, in this case, capacity
 455 was 450 g for 30 minutes.

456 The mixing procedure was the same for the TCC, GCC and ECC systems, and only mixing time differed.
 457 As explained in Section 2.2 “Experimental procedure”, an AEG SBE705RE power drill connected to a
 458 paint mixer was used for samples preparation. This power drill works at 0.705 kW and the capacity for
 459 each mix cycle was 0.012 m³. For the CA samples the mixing time lasted 150 seconds (2.5 minutes), but
 460 it was 120 seconds (2 minutes) for the GCC and ECC systems.

461 For these calculations, and as with the mill and mix procedures, we took the national average value
 462 provided by IDAE as the emission factor of energy use, which is 0.25 kg CO₂ per kWh⁴⁵.

463 With these considerations, the calculations of the emissions associated with the manufacture that
 464 corresponded to each sample were made by Equation (7) and the results were: $E_{M,CA} = 0.6$ kg CO₂/m³
 465 CA, $E_{M,FR} = 34$ kg CO₂/m³ FR, $E_{M,SR} = 37.5$ kg CO₂/m³ SR, $E_{M,FRR} = 32.1$ kg CO₂/m³ FRR and $E_{M,SRR} =$
 466 37.1 kg CO₂/m³ SRR.

467 Figure 5 shows a comparison of the CO₂ emissions from the different materials and operations for each
 468 concrete. Calculated kg of CO₂ per m³ of material, the relative values are plotted and absolute values are
 469 provided.

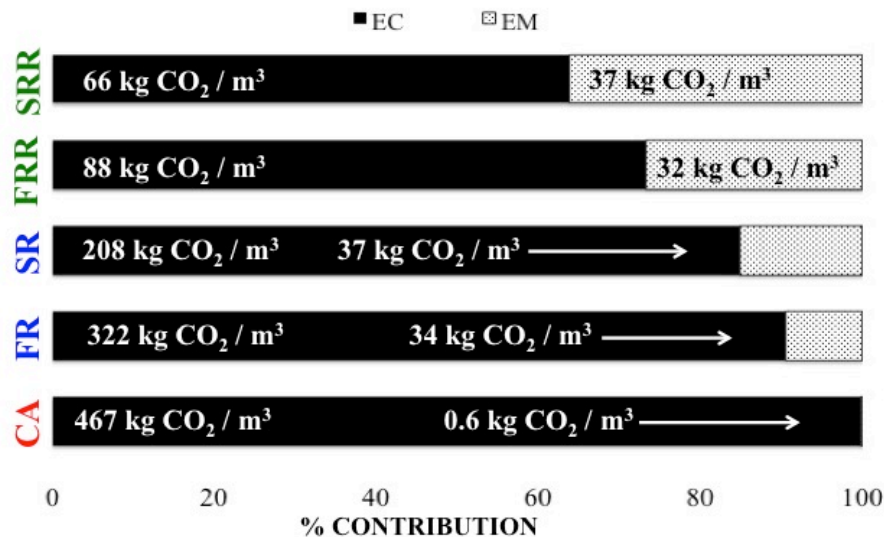


Fig 5. Comparison of the relative CO₂ emissions contributions from the components (EC) and manufacture processes (EM) for the CA, FR, SR, FRR and SRR cellular concretes. The absolute CO₂ emissions values are given in each bar.

470 As we can see, no influence of the TCC manufacture process was perceived, and total emission was
 471 related mainly to its components. However, as in both the GCC and ECC systems, manufacturing
 472 influenced the total CO₂ emissions. Indeed the effect of the milling procedure was more important than
 473 the mixing procedure for all the samples. An analysis of the results revealed that: $E_{M,FR}$ represents 9.5%,
 474 with 97.5% from milling and 2.5% from mixing; $E_{M,SR}$ represents 15.3%, with 97.7% from milling and
 475 2.3% from mixing; $E_{M,FRR}$ represents 26.7%, with 97.3% from milling and 2.7% from mixing; $E_{M,SRR}$
 476 represents 31.1%, with 97.7% from milling and 2.3% from mixing. The absolute CO₂ emissions
 477 produced from manufacturing were higher when the required solid material increased (Table 5) due to
 478 the high-energy requirement of pre-treatment.

479 These results can be explained because, nowadays for TCC, an industrial process of OPC and A
 480 manufacturing exists, and no pre-treatment in laboratory is required. If the same conditions for GCC and
 481 ECC systems could be considered, the emissions of this materials would be lower.

482 Finally, the resultant carbon footprint of each material was calculated by Equation (8). Figure 6 shows a
 483 comparison of the total CO₂ emissions from the CA, FR, SR, FRR and SRR cellular concretes analysed
 484 in the present study.

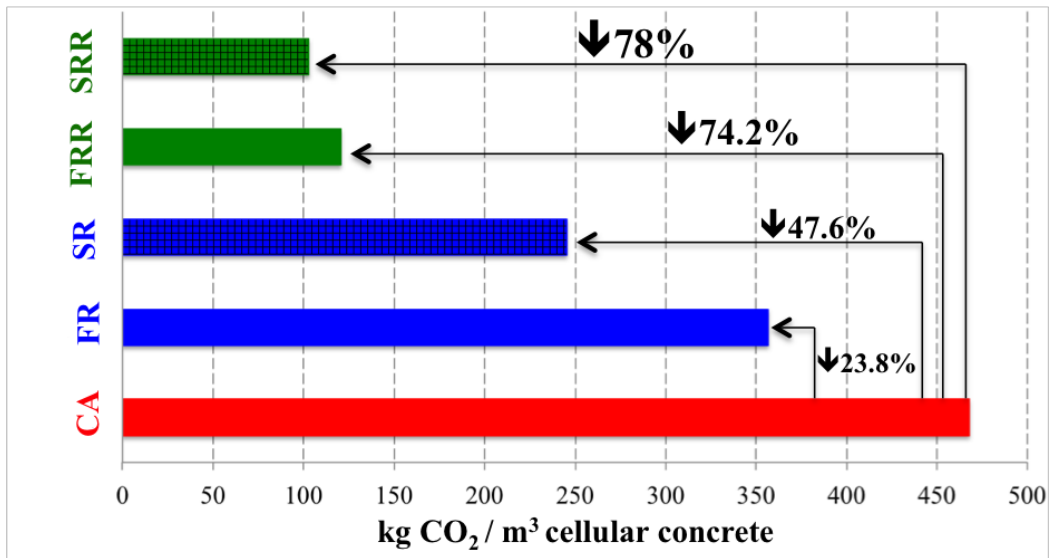


Fig 6. The total CO₂ emissions associated with cellular concretes CA, FR, SR, FRR and SRR and reductions in CO₂ emissions compared to the CA sample (the TCC system).

485 For TCC, total emissions were 467.6 kg CO₂/m³ CA. For GCC, where OPC and A were replaced with
 486 alternative raw materials (FCCRM and BFSRM, respectively), the total CO₂ emissions significantly
 487 reduced: i) the total emissions for the FR sample were 356.5 kg CO₂/m³ FR, which is 23.8% lower than
 488 those for the CA sample; ii) for the SR sample, they were 245.2 kg CO₂/m³ SR, 47.6% lower than those
 489 for CA. The last development step, where commercial waterglass was replaced by RHA (ECC systems),
 490 gave a relevant reduction in the total carbon footprint: 66.2% vs. FR and 74.2% vs. CA for the FRR
 491 system (120.4 kg CO₂/m³ FRR), and 58% vs. SR and 78% vs. CA for the SRR systems (102.9 kg CO₂/m³
 492 SRR).

493 5. CONCLUSIONS

494 In this research, the density of the proposed alternative cellular concrete (FR, FRR, SR and SRR) was
 495 lower than 1000 kg/m³, which represents suitable lightweight insulation behaviour. Besides, mechanical
 496 behaviour came close to TCC in all the evaluated alternative cellular concretes.

497 The obtained results for the new proposed ECC demonstrated the high effectiveness of soluble silica
 498 from RHA to replace the silica from WG. Replacing the traditional alkaline solution by a mixture of
 499 RHA and NaOH allowed new cellular concrete to be prepared with similar properties to those found for
 500 the equivalent systems with WG. This implies an interesting chance to reduce the use of synthetic
 501 chemical reagents for preparing this cellular concrete type.

502 The results of the carbon footprint calculations revealed that with the new ECC it is possible to minimise
 503 CO₂ emissions by more than 70% versus TCC emissions. The factors that most contributed to the carbon
 504 footprint were: i) the OPC in TCC; ii) WG as well as milling in the GCC systems; iii) only milling in the
 505 ECC systems. Calculations were made by considering laboratory conditions: if the industrial milling of
 506 the alternative raw materials required for the GCC and ECC systems manufacturing could be considered,
 507 the emissions from milling would be much lower. For the GCC systems, the contribution of commercial
 508 waterglass (WG) was more than 80%. Indeed the new alternative ECC allowed the possibility of reducing
 509 greenhouse gas emissions and contributing to sustainable development by integrating green chemistry
 510 principles into construction materials by reusing wastes, including those related to aluminium-based gas
 511 generators.

512 **Acknowledgements**

513 The authors acknowledge the financial support from the Universitat Politècnica de València (UPV)
514 through internal project GEOCELPLUS. The authors like also to express special grateful to Dra. Mrs.
515 Josefa L. Roselló Caselles for recycled aluminium foil, and to the Electronic Microscopy Service of the
516 UPV. Thanks are given to DACSA, Cementval and BPOil for supplying samples.

517 **Bibliography**

518

- 519 1 O. Ortiz, F. Castells and G. Sonnemann, *Constr. Build. Mater.*, 2009, **23**, 28–39.
- 520 2 L. F. Cabeza, L. Rincón, V. Vilariño, G. Pérez and A. Castell, *Renew. Sustain.*
521 *Energy Rev.*, 2014, **29**, 394–416.
- 522 3 M. Jiang, X. Chen, F. Rajabipour and C. T. Hendrickson, *J. Infrastruct. Syst.*,
523 2014, **20**, 1–9.
- 524 4 K. Cavanaugh and J. F. Speck, *Concrete*, 2002, 1–21.
- 525 5 N. Narayanan and K. Ramamurthy, *Cem. Concr. Compos.*, 2000, **22**, 321–329.
- 526 6 Z. Zhang, J. L. Provis, A. Reid and H. Wang, *Constr. Build. Mater.*, 2014, **56**,
527 113–127.
- 528 7 H. Esmaily and H. Nuranian, *Constr. Build. Mater.*, 2012, **26**, 200–206.
- 529 8 R. Arellano Aguilar, O. Burciaga Díaz and J. I. Escalante García, *Constr. Build.*
530 *Mater.*, 2010, **24**, 1166–1175.
- 531 9 T. W. Bremner, P. M. Carkner, M. Healy and A. Litvin, *Man. Concr. Pract.*,
532 1997, 2–6.
- 533 10 D. K. Panesar, *Constr. Build. Mater.*, 2013, **44**, 575–584.
- 534 11 B. Dolton and C. Hannah, 2006, 1–11.
- 535 12 K. L. Scrivener and R. J. Kirkpatrick, *Cem. Concr. Res.*, 2008, **38**, 128–136.
- 536 13 E. Gartner, *Cem. Concr. Res.*, 2004, **34**, 1489–1498.
- 537 14 A. Palomo and J. I. López de la Fuente, *Cem. Concr. Res.*, 2003, **33**, 281–288.
- 538 15 P. Duxson, J. L. Provis, G. C. Lukey and J. S. J. van Deventer, *Cem. Concr. Res.*,
539 2007, **37**, 1590–1597.
- 540 16 P. J. Davidovits, *Geopolymer 2002 Conf.*, 2002, 1–16.
- 541 17 J. Davidovits, *First Int. Conf. Alkaline Cem. Concr.*, 1994, 131–149.
- 542 18 A. Font, M. V. Borrachero, L. Soriano, J. Monzó and J. Payá, *J. Clean. Prod.*,
543 2017, **168**, 1120–1131.

- 544 19 J. L. Provis, *Cem. Concr. Res.*, , DOI:10.1016/j.cemconres.2017.02.009.
- 545 20 A. Mellado, C. Catalán, N. Bouzón, M. V. Borrachero, J. M. Monzó and J. Payá,
546 *RSC Adv.*, 2014, **4**, 23846–23852.
- 547 21 L. K. Turner and F. G. Collins, *Constr. Build. Mater.*, 2013, **43**, 125–130.
- 548 22 J. R. Dodson, E. C. Cooper, A. J. Hunt, A. Matharu, J. Cole, A. Minihan, J. H.
549 Clark and D. J. Macquarrie, *Green Chem.*, 2013, **15**, 1203.
- 550 23 N. Bouzón, J. Payá, M. V. Borrachero, L. Soriano, M. M. Tashima and J. Monzó,
551 *Mater. Lett.*, 2014, **115**, 72–74.
- 552 24 J. C. B. Moraes, A. Font, L. Soriano, J. L. Akasaki, M. M. Tashima, J. Monzó,
553 M. V. Borrachero and J. Payá, *Constr. Build. Mater.*, ,
554 DOI:10.1016/j.conbuildmat.2018.03.230.
- 555 25 M. Torres-Carrasco and F. Puertas, *J. Clean. Prod.*, 2015, **90**, 397–408.
- 556 26 EST: Publications,
557 [http://www.fao.org/economic/est/publications/publicaciones-sobre-el-](http://www.fao.org/economic/est/publications/publicaciones-sobre-el-#WrfjcGYrw_U)
558 [#WrfjcGYrw_U](http://www.fao.org/economic/est/publications/publicaciones-sobre-el-#WrfjcGYrw_U), (accessed 25 March 2018).
- 559 27 J. C. Marchal, D. J. Krug III, P. McDonnell, K. Sun and R. M. Laine, *Green*
560 *Chem.*, 2015, **17**, 3931–3940.
- 561 28 T. Luukkonen, Z. Abdollahnejad, J. Yliniemi, P. Kinnunen and M. Illikainen, *J.*
562 *Clean. Prod.*, 2018, **187**, 171–179.
- 563 29 R. U. Ayres, 1995, 24.
- 564 30 U.S. Department of Energy, *Ind. Technol. Progr. Energy Effic. Renew. Energy*,
565 2007, 150.
- 566 31 Arpal Asociacion para el Reciclado de Aluminio.
- 567 32 E. G. de Araújo and J. A. S. Tenório, *Mater. Sci. Forum*, 2005, **498–499**, 198–
568 204.
- 569 33 European Aluminium Foil Association, Did you know? - EAFA - The home of
570 aluminium foil.
- 571 34 J. Payá, J. Monzó and M. V. Borrachero, *Cem. Concr. Res.*, 1999, **29**, 1773–
572 1779.
- 573 35 J. C. B. Moraes, M. M. Tashima, J. L. Akasaki, J. L. P. Melges, J. Monzó, M. V.
574 Borrachero, L. Soriano and J. Payá, *Constr. Build. Mater.*, 2016, **124**, 148–154.
- 575 36 E. Muthu Kumar and K. Ramamurthy, *Constr. Build. Mater.*, 2017, **156**, 1137–
576 1149.
- 577 37 J. Payá, M. V. Borrachero, J. Monzó and L. Soriano, *Mater. Construcción*, 2009,

- 578 **59**, 37–52.
- 579 38 ASTM International, ASTM D5334 - 14 Standard Test Method for
580 Determination of Thermal Conductivity of Soil and Soft Rock by Thermal
581 Needle Probe Procedure.
- 582 39 IEEE 442-1981 - IEEE Guide for Soil Thermal Resistivity Measurements.
- 583 40 S. Eggleston, L. Buendia, K. Miwa, T. Ngara and K. Tanabe, *2006 IPCC Guidel.*
584 *Natl. Greenh. Gas Invent.*, 2006, 6.
- 585 41 A. J. Hamad, *Int. J. Mater. Sci. Eng.*, 2014, **2**, 152–157.
- 586 42 E. K. K. Nambiar and K. Ramamurthy, *Cem. Concr. Res.*, 2007, **37**, 221–230.
- 587 43 a Mellado, C. Catalán, N. Bouzón, M. V Borrachero, J. M. Monzó and J. Payá,
588 *RSC Adv.*, 2014, **4**, 23846–23852.
- 589 44 M. Torres-Carrasco, C. Rodríguez-Puertas, M. Del Mar Alonso and F. Puertas,
590 *Bol. la Soc. Esp. Ceram. y Vidr.*, 2015, **54**, 45–57.
- 591 45 S. Ministerio de Industria, Energía y Turismo, Secretaría de Estado de Energía,
592 Madrid, IDAE 2011, <http://www.idae.es/>, (accessed 12 March 2018).
- 593